


Cite this: *RSC Adv.*, 2023, 13, 24286

Received 8th June 2023
Accepted 7th August 2023
DOI: 10.1039/d3ra03833e

rsc.li/rsc-advances

Synthesis and mechanical performance of thermoformable cellulose fatty acid esters using natural soap†

Tessei Kawano^a and Yoshito Andou  ^{*ab}

A cellulose fatty acid ester consisting solely of natural organic compounds is synthesized by heterogeneous esterification. Solid soap, a natural product-based compound, is used as a mixed fatty acid source. The synthesized cellulose ester can be readily processed into a semi-transparent film. Mechanical properties of the cellulose ester are also investigated.

Plastics have played an irreplaceable role in the manufacturing industry and our daily life. However, the current industrial production of plastics heavily depends on petroleum chemicals. As a result, there are widespread concerns about environmental issues and the depletion of fossil resources due to the enormous production and inefficient management of petroleum-based plastics. To address these global challenges, renewable polymers derived from natural resources have drawn attention as promising alternatives to non-renewable petrochemical-based materials.^{1–3} Cellulose, available from non-edible biomass sources, is known as the most abundant and virtually inexhaustible natural polymer on earth.^{4,5} Owing to its biodegradability, crystallinity, and thermal stability, cellulose has gained much attention as a starting material for the fabrication of bio-based plastics. Nevertheless, cellulose is insoluble in most organic solvents and does not possess thermoplastic properties unlike conventional plastics due to its intrinsically hydrophilic nature and the formation of strong inter- and intramolecular hydrogen bonds.^{6,7} Therefore, overcoming the lack of processability of cellulose has been considered the key issue for the development of cellulose-based materials as a substitute for petroleum-based plastics.

Cellulose derivatives, in which hydroxyl groups of cellulose are substituted by other functional groups, have the potential to overcome the drawback of cellulose. Starting with cellulose nitrate reported in the 1870s, a variety of cellulose derivatives have been developed to date through various chemical reactions

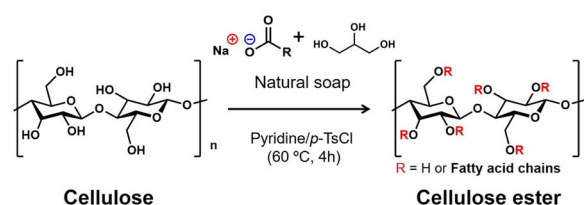
such as esterification,^{8,9} etherification,¹⁰ and graft copolymerization.¹¹ Among them, cellulose esters including cellulose acetate, cellulose acetate propionate, and cellulose acetate butyrate are the most commercially important cellulose-based bioplastics in various applications such as coatings,^{12,13} films, optical device,¹⁴ and so forth. However, such short-chain cellulose esters have poor thermal processability due to their narrow processing window represented by the gap between glass transition/melting temperature and degradation temperature. Therefore, additional plasticizers are often required for thermoforming.^{15,16} Facing this problem, cellulose esters with the chain length of fatty acid substituent >6, known as long-chain cellulose esters, have attracted considerable interest as cellulose-based bioplastics with improved thermal processability.^{17–19} Cellulose esters containing long-chain fatty acid in their side chains could be the most promising candidates for the next generation of bioplastics.

Herein, a thermoformable cellulose derivative, which has not been reported before, was synthesized with microcrystalline cellulose (MCC) and natural soap as a mixed fatty acid source through heterogeneous esterification in pyridine/*p*-toluenesulfonyl chloride (*p*-TsCl) medium (Scheme 1). Natural soap derived from natural resources contains glycerol and sodium salts of structurally diverse fatty acids, such as oleic acid, lauric acid, stearic acid, and palmitic acid. The effective use of natural soap has been highly required from the perspective of

^aDepartment of Life Science and Systems Engineering, Graduate School of Life Science and Systems Engineering, Kyushu Institute of Technology, 2-4 Hibikino, Wakamatsu-ku, Kitakyushu, Fukuoka 808-0196, Japan. E-mail: kawano.tessei758@mail.kyutech.jp

^bCollaborative Research Centre for Green Materials on Environmental Technology, Kyushu Institute of Technology, 1-1 Sensui-chou, Tobata-ku, Kitakyushu, Fukuoka 804-8550, Japan. E-mail: yando@life.kyutech.ac.jp

† Electronic supplementary information (ESI) available: Experimental details and additional Fig. S1–S6 and Tables S1 and S2. See DOI: <https://doi.org/10.1039/d3ra03833e>



Scheme 1 Synthesis of fatty acid cellulose ester.



sustainable resources.^{20,21} The synthesized cellulose esters were abbreviated as MCC-MFA_*n* in which *n* represented the weight ratio of natural soap to MCC. Furthermore, sodium oleate, sodium stearate, and the mixture of these fatty acid salts were also used to synthesize cellulose esters, labeled MCC-C18:1, MCC-C18, and MCC-C18:1/C18, respectively, as references. The procedure followed is in detail described in the ESI† and the amounts of each reagent used are shown in Table S1.†

Fourier transform infrared (FT-IR) confirmed the successful substitution of hydroxy groups, as indicated by the decrease in intensity of the broad peak at 3100–3600 cm^{−1} assigned to the O–H stretching and the appearance of the peak at 1751 cm^{−1} and 2800 to 2900 cm^{−1} attributed to C=O stretching of esters and C–H stretching of alkyl chains, respectively (Fig. 1). Besides, the absorbance peak at 3006 cm^{−1} assigned to the =C–H stretching was confirmed in MCC-C18:1, MCC-C18:1/C18, and MCC-MFA samples suggesting the presence of unsaturated fatty acids in their side chains.²² Comparing the cellulose esters synthesized with the different weight ratios of natural soap, it can be seen that the intensity of the peak at 3400 cm^{−1} is higher in MCC-MFA₁₀ and MCC-MFA₄. This indicates that the amount of natural soap added affects the esterification reaction, and agrees with the yield trend, which was MCC-MFA₆ > MCC-MFA₈ > MCC-MFA₄ > MCC-MFA₁₀ (Table S1†). In addition to the FTIR analysis, chloroform-soluble fraction of each prepared cellulose ester was characterized by proton nuclear magnetic resonance (¹H-NMR) spectroscopy to further elucidate the chemical structure (Fig. S1†). Although a degree of substitution (DS) of 2.3 to 2.5 was calculated from the ¹H-NMR spectra of all samples, the amount of chloroform-soluble fraction of MCC-MFA₁₀ was 7.4%, which was lower than that of the other samples, 17 to 20%.

Since the esterification reaction of glycerol and fatty acids proceeds competitively during the derivatization of cellulose, the increased amount of natural soap also increased the acid catalyst consumed to produce triglycerides. Therefore MCC-MFA₁₀ obtained in the lowest yield.

The thermal behavior of cellulose esters was analyzed using thermogravimetric analysis (TGA) and differential scanning calorimetry (DSC). Initial weight loss at 80 to 100 °C occurred due to the removal of water, which is absent in all cellulose esters, indicating the hydrophobic nature of the synthesized derivatives (Fig. S2†). Besides, the onset degradation temperature (*T*_{d-5%}) decreased compared to the pristine MCC due to the loss of crystallinity caused by substitution with long fatty acid chains and partial decomposition of cellulose, but still retained a high degradation temperature of about 230 °C (Table S2†). In addition, cellulose esters showed a slight weight loss at 300 to 400 °C attributed to thermal degradation of cellulose backbone, while first weight loss is due to the decomposition of grafted fatty acid chain. Fig. 2 shows DSC curves in 2nd heating of cellulose esters. An endothermic peak attributed to the melting temperature (*T*_m) of crystals formed by a part of alkyl-side chains was observed in only MCC-C18 and MCC-C18:1/C18 at 30.0 and −8.7 °C, respectively. The most probable reason is that the presence of stearyl groups with a linear structure results in better alignment and orientation of the side chains. Similar thermal behavior has been confirmed by DSC analysis for cellulose esters with linear substituent length of 10 or more.²³ MCC-MFA samples exhibited multiple glass transition temperatures (*T*_g), which varied depending on the weight ratio of the natural soap to MCC, suggesting that fatty acid side chains with diverse structures have been introduced (Table S2†). More specifically *T*_g at below 0 °C and around 60 °C correspond to the segmental motion of side chains and cellulose backbones, respectively.

Fig. 3 and S3† depicts the X-ray diffraction (XRD) patterns. MCC showed the typical cellulose I crystal structure composed of (1–10), (110), (200), and (004) lattice planes. On the other hand, XRD spectra of cellulose esters consist mainly of two peaks observed in the region 2θ = 2°–4° and 18°–22°. The former is overlapped peak composed of amorphous regions and crystalline moieties formed by long alkyl side chains, while the diffraction peak in the low angle region is originated from the planar arrangement of parallel cellulosic backbone chains.²⁴

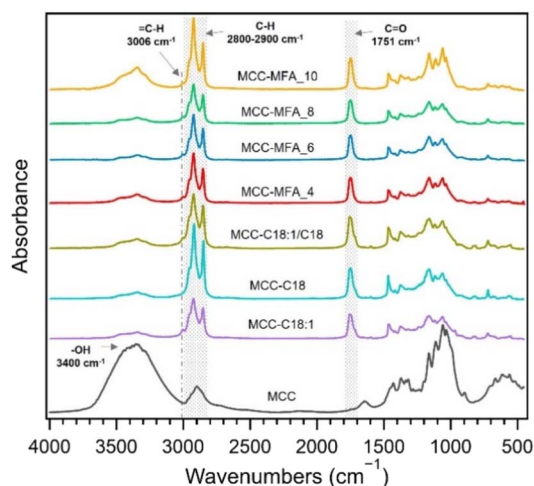


Fig. 1 FT-IR spectra of synthesized cellulose esters.

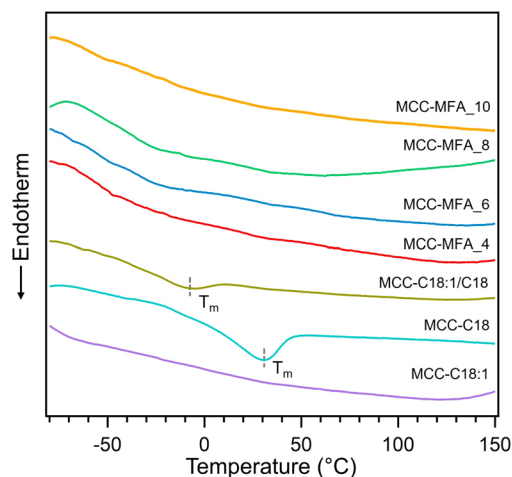


Fig. 2 DSC curves of cellulose esters.

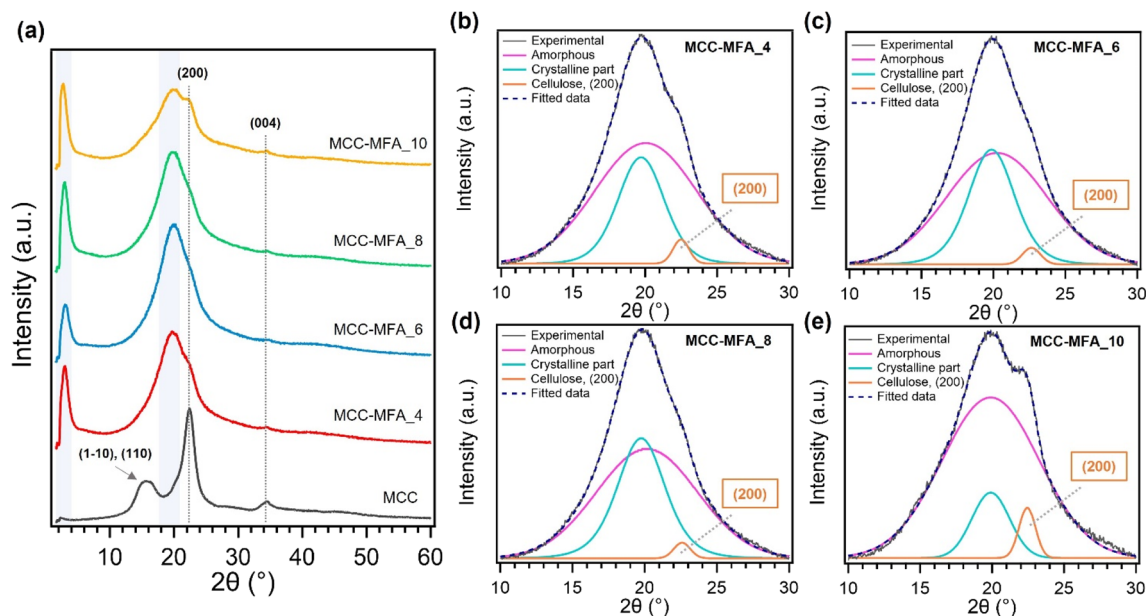


Fig. 3 (a) XRD profiles of MCC and MCC-MFA samples; (b)–(e) deconvoluted peaks superimposed on the experimental curves for MCC-MFA samples.

The substitution with long chains can permanently prevent cellulose from regular arrangement and leads to an increase in the amorphous content, thus MCC and the synthesized cellulose esters showed completely different XRD patterns. In the deconvoluted peaks of XRD patterns for MCC-MFA samples, the remaining diffraction peaks assigned to the (200) lattice plane of cellulose I were confirmed (Fig. 3b–e). These peaks are more prominent in MCC-MFA₁₀ and MCC-MFA₄, suggesting the less substitution as indicated by chemical structure analysis and the yield. Furthermore, MCC-MFA₁₀ showed minimal formation of crystalline moiety by side chains due to the less introduction of fatty acid chains. The synthesized cellulose esters were also exhibited the different surface morphology as compared with the unmodified cellulose. The pristine MCC showed a rod-like morphology due to the agglomeration of cellulose fibrils and hydrolysis during the manufacturing process (Fig. S4†). In contrast, sheet-like morphology was observed for the cellulose esters, which is likely due to the less crystalline and agglomeration caused by the substitution of hydroxyl groups with long chains. In addition, the weight ratio of MCC and natural soap affected the morphology and MCC-MFA₁₀, with lowest yield, showed insignificant change in morphology as compared to MCC.

Thermal processability has been highly required for the utilization of cellulose derivatives as an alternative to petroleum-based plastics. Long-chain cellulose esters synthesized in this work were thermal processable, in which all samples were able to be formed into semi-transparent films by hot-pressing method at 120 °C and 10 MPa (Fig. 4a). Interestingly, the films prepared from MCC-MFA samples were colorless, while hot-pressed films of MCC-C18:1 and MCC-C18 were slightly yellowish. In general, cellulose esters synthesized using the pyridine/*p*-TsCl medium have shown yellow or slight brown

color, likely due to the oxidation of the cellulose molecules and side reactions caused by the excess *p*-TsCl.²⁵ Therefore, it can be expected that the excess amounts of acids were consumed by the glycerol contained in the natural soap, and discoloration of the cellulose ester was suppressed. Indeed, the colorless film

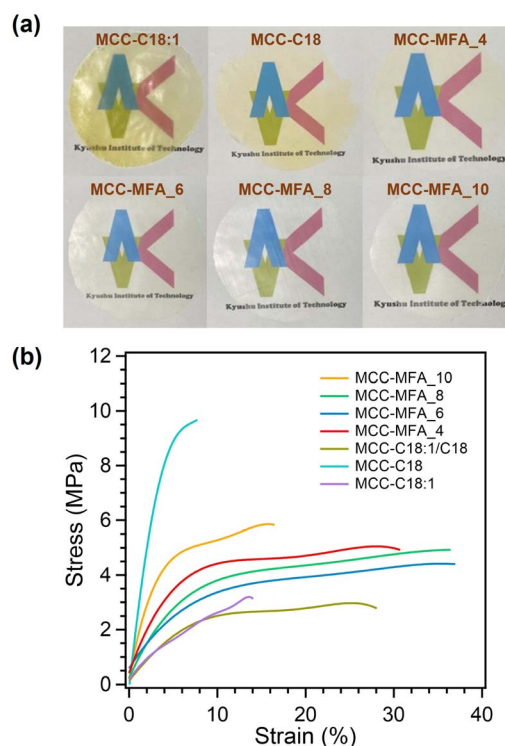


Fig. 4 (a) Representative images and (b) stress–strain curves of hot-pressed cellulose ester films.



was obtained from the MCC-C18:1/C18 containing glycerol that was intentionally added during the synthesis process (Fig. S5a†). This result demonstrates the advantage of our cellulose esters with repressed discoloration caused by esterification and thermal processing. Furthermore, it is revealed that thermoformed film of MCC-C18:1/C18 synthesized under the presence of glycerol possess better mechanical properties than that of MCC-C18:1/C18 (Fig. S5b†). In addition, MCC-MFA films possess hydrophobic surfaces, with a water contact angle of greater than 100°, and hydrophobicity of cellulose ester films depend on the reaction conditions and structure of side chains (Fig. S6†). The mechanical properties of cellulose esters were evaluated by tensile test. As shown in Fig. 4b and Table S3,† MCC-MFA samples exhibited higher toughness than that of cellulose esters prepared with sodium oleate, sodium stearate, or the mixture of these fatty acid salts, particularly MCC-MFA_4 demonstrated the greatest toughness of 1.33 J m⁻³. Besides, MCC-MFA_10 showed the highest tensile strength of 60.6 MPa and Young's modulus of 1.24 GPa among the MCC-MFA samples, which could be explained by the remained cellulose I crystal structure and the less substitution revealed by FT-IR and XRD analyses. On the other hand, MCC-MFA_6 and MCC-MFA_8 obtained in relatively high yields, showed high elongation at break of 34.65 and 33.19%, respectively. The rigid and brittle property of MCC-C18 is due to the well-aligned linear alkyl chain of stearyl moieties. Moreover, a comparison study with other long-chain cellulose esters revealed that MCC-MFA samples possess better or comparable tensile strength and elongation to those of previously reported cellulose palmitate and cellulose oleate with a DS of 0.9 to 3.0 (Fig. S7†). However, as compared to cellulose esters with low DS and with relatively short side chains, the mechanical properties of MCC-MFA samples were still inferior. Therefore, the enhancement of mechanical performance by controlling the substitution degree, incorporation of fillers, and post-treatment on cellulose ester films would be a topic in future publication.

In conclusion, cellulose derivatives with structurally diverse fatty acid side chains were synthesized through the heterogeneous esterification using commercially available natural soap. Chemical and crystal structure analyses, as well as comparison with cellulose oleate and cellulose stearate, confirmed that fatty acids in natural soap were successfully grafted on cellulose. The synthesized MCC-MFA samples maintained the good thermal stability with $T_{d-5\%}$ of around 240 °C, while they were moldable into a semi-transparent film by hot-pressing process at 120 °C. This ensured that MCC-MFA samples have the excellent processing windows which are highly required for industrial production of polymeric materials. The weight ratio of natural soap to MCC significantly affected the mechanical properties of MCC-MFA films. MCC-MFA_4 showed the highest toughness among the synthesized cellulose esters, suggesting that a 1 : 4 ratio of MCC and natural soap would be the optimal conditions for this particular work. Comparison with previously reported long-chain cellulose esters revealed that MCC-MFA samples possess comparable tensile strength and elongation at break to cellulose palmitate and cellulose oleate with high DS. Furthermore, it was first discovered that glycerol in natural soap can

prevent discoloration of cellulose esters during esterification and processing. We believe that such cellulose esters could potentially replace petroleum-based plastics in a variety of fields where thermal processability is required.

Conflicts of interest

There are no conflicts to declare.

Notes and references

- 1 Y. Hu, W. Zhu, K. Song and Z. Yu, *Mater. Lett.*, 2022, **321**, 132421.
- 2 A. K. Mohanty, F. Wu, R. Mincheva, M. Hakkarainen, J. M. Raquez, D. F. Mielewski, R. Narayan, A. N. Netravali and M. Misra, *Nat. Rev. Methods Primers*, 2022, **2**, 46.
- 3 L. Zhu, B. Dang, K. Zhang, J. Zhang, M. Zheng, N. Zhang, G. Du, Z. Chen and R. Zheng, *ACS Sustainable Chem. Eng.*, 2022, **10**, 13775–13785.
- 4 A. Sato, D. Kabusaki, H. Okumura, T. Nakatani, F. Nakatsubo and H. Yano, *Composites, Part A*, 2016, **83**, 72–79.
- 5 T. Kawano, S. Iikubo and Y. Andou, *Polymers*, 2021, **13**, 4450.
- 6 C. Tsiptsias, E. G. Nikolaidou, X. Ntampou, I. Tsvintzelis and C. Panayiotou, *Thermochim. Acta*, 2022, **707**, 179106.
- 7 E. Esen, P. Hädinger and M. A. R. Meier, *Biomacromolecules*, 2021, **22**, 586–593.
- 8 J. Lease, T. Kawano and Y. Andou, *Polymers*, 2021, **13**, 4397.
- 9 J. Wang, L. Emmerich, J. Wu, P. Vana and K. Zhang, *Nat. Sustain.*, 2021, **4**, 877–883.
- 10 E. Saiki, M. Yoshida, K. Kurahashi, H. Iwase and T. Shikata, *ACS Omega*, 2022, **7**, 28849–28859.
- 11 E. Lizundia, E. Fortunati, F. Dominici, J. L. Vilas, L. M. León, I. Armentano, L. Torre and J. M. Kenny, *Carbohydr. Polym.*, 2016, **142**, 105–113.
- 12 K. Jin, J. Zhang, W. Tian, X. Ji, J. Yu and J. Zhang, *ACS Sustainable Chem. Eng.*, 2020, **8**, 5937–5945.
- 13 S. Zhang, W. Li, W. Wang, S. Wang and C. Qin, *Appl. Surf. Sci.*, 2019, **497**, 143816.
- 14 Z. Lang, Y. Ju, Y. Wang, Z. Xiao, H. Wang, D. Liang, J. Li and Y. Xie, *Chem. Eng. J.*, 2022, **435**, 134851.
- 15 N. A. Mostafa, A. A. Farag, H. M. Abo-dief and A. M. Tayeb, *Arabian J. Chem.*, 2018, **11**, 546–553.
- 16 S. Hu, X. Liu, M. Zhang, Y. Wei, R. Qi, Y. Zhu and S. Chen, *Cellulose*, 2022, **29**, 7849–7861.
- 17 S. Guzman-Puyol, G. Tedeschi, L. Goldoni, J. J. Benítez, L. Ceseracciu, A. Koschella, T. Heinze, A. Athanassiou and J. A. Heredia-Guerrero, *Food Hydrocolloids*, 2022, **128**, 107562.
- 18 D. F. Hou, M. L. Li, C. Yan, L. Zhou, Z. Y. Liu, W. Yang and M. B. Yang, *Green Chem.*, 2021, **23**, 2069–2078.
- 19 M. Jebrane, N. Terziev and I. Heinmaa, *Biomacromolecules*, 2017, **18**, 498–504.
- 20 M. R. Chirani, E. Kowsari, T. Teymourian and S. Ramakrishna, *Sci. Total Environ.*, 2021, **796**, 149013.
- 21 P. Muanruksa, P. Wongsirichot, J. Winterburn and P. Kaewkannetra, *Biomass Bioenergy*, 2021, **154**, 106231.



- 22 F. Y. Huang, Y. Yu and X. J. Wu, *Adv. Mater. Res.*, 2011, **197**–**198**, 1306–1309.
- 23 P. Willberg-Keyriläinen, J. Vartiainen, A. Harlin and J. Ropponen, *Cellulose*, 2017, **24**, 505–517.
- 24 L. Duchatel-Crépy, N. Joly, P. Martin, A. Marin, J. F. Tahon, J. M. Lefebvre and V. Gaucher, *Carbohydr. Polym.*, 2020, **234**, 115912.
- 25 M. Chen, R. M. Li, T. Runge, J. Feng, J. Feng, S. Hu and Q. S. Shi, *ACS Sustainable Chem. Eng.*, 2019, **7**, 16971–16978.

